Separation of Dielectric Nonideality from Preferential Solvation in Binary Solvent Systems: An Experimental Examination of the Relationship between Solvatochromism and Local Solvent Composition around a Dipolar Solute

Mazdak Khajehpour, Carrie M. Welch, Keith A. Kleiner, and John F. Kauffman*

Department of Chemistry, University of Missouri−Columbia, Columbia, Missouri 65211-7600

Received: March 5, 2001

Dielectric nonideality of a binary solvent system refers to the deviation of the Onsager reaction field function from linearity in the polar mole fraction of the solvent mixture. A dipolar fluorophore dissolved in an ideal dielectric mixture exhibits a solvatochromic shift that is linear in the solvent polar mole fraction in it's solvation sphere. As a result, the "local composition" can be easily determined from the peak shift. Here we identify the conditions under which this linear approximation is appropriate for estimating local compositions around dipolar solutes. In a previous study (Khajehpour, M. H.; Kauffman, J. F. *J. Phys. Chem. A* **2000**, *104*, 7151−7159), we have demonstrated the influence of dielectric nonideality on the observed emission peak shifts of the charge-transfer excited state of ADMA [1-(9-anthryl)-3-(4-*N*,*N*-dimethylaniline)propane] in hexanes−ethanol mixtures. The linear approximation fails for this binary solvent, and a more elaborate method of analysis such as Suppan's nonlinearity ratio method must be used to determine the local composition from solvatochromic shifts. In this work, we examine mixture nonideality and dielectric enrichment in hexane−tetrahydrofuran and hexane−dichloromethane mixtures. Our analysis demonstrates that the contribution of nonideality to the observed solvatochromic shifts cannot be neglected in these binary solvents. Using Suppan's theory of dielectric enrichment, we have calculated the local composition of ADMA's solvation sphere and find that it is enriched in the polar component by ∼30% over the bulk composition. This calculated value agrees with experimental measures of the local composition based on analysis of solvatochromic shifts using Suppan's nonlinearity ratio method which accounts for dielectric nonideality. The linear approximation overpredicts this composition by as much as 50%, even though these binary solvents are more nearly ideal than the hexane−ethanol system. Following this observation, we have identified conditions under which the linear approximation is justified, and find that for most cases of practical importance the linear approximation will not provide accurate estimates of the local solvent composition from solvatochromic studies. Similarly, solvatochromic shifts can only be accurately predicted from theoretical local compositions if dielectric nonideality is taken into account. These results along with our previous studies indicate that the charge-transfer excited state of ADMA behaves as an ideal dipolar solute.

I. Introduction

When a polar solute is dissolved in a binary solvent mixture it interacts differently with each of the solvent components. This difference in interaction causes the solvent composition in the near vicinity of the solute to be different from the bulk. This concept of preferential solvation has long been used qualitatively to rationalize measured solute properties that deviate from a linear dependence on solvent composition.[1] Spectroscopic measurements are normally influenced only by short-range interactions making them well suited for characterizing the local environment of the solute. Preferential solvation is often correlated with spectral measurements using the expression[2−9]

$$\delta_{AB} = y_A\delta_A + y_B\delta_B \qquad (1)$$

in which δ_A and δ_B are spectral properties (peak positions, peak intensities, kinetic rate constants, etc.) of the solute measured in neat solvents A and B while δ_{AB} is the same property measured in the binary solvent mixture of A and B. The parameters y_A and $y_B = 1 - y_A$ are considered to be the local compositions of the solvent components near the solute. Equation 1 offers a simple methodology for calculating local compositions. However there is no theoretical justification for assuming that δ_{AB} is a mol fraction weighed average of δ_A and δ_B.[9−11] In fact Ben-Naim points out that in general, eq 1 will result in different values of y_A for different kinds of spectroscopic measurements on the same chemical system. The use of spectroscopic methods for this purpose requires a correct understanding of the dependence of the measured signal upon the local composition.

Solvatochromic shifts are often observed in the electronic spectra of chromophoric solutes. These shifts reflect the extent of stabilization that the molecular ground and excited states experience due to solvent−solute interactions. If the solute molecule is modeled as a dipole immersed in a continuum dielectric, expressions for the stabilization of the dipole can be obtained. Solvatochromic shifts in neat solvents have often been correlated with expressions obtained from these continuum models.[12] Binary solvent mixtures can also be represented by a continuum dielectric, and Suppan and co-workers have successfully formulated preferential solvation in terms of the

* To whom correspondence should be addressed. E-mail: kauffmanj@missouri.edu.

10.1021/jp010825a CCC: $20.00
Published on Web 05/10/2001

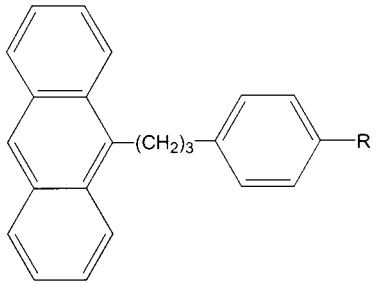

Figure 1. Structure of ADMA [R═N(CH$_3$)$_2$] and APP (R═H). See Figure 3 for representative structures.

dielectric enrichment model.[13−16] This model provides a theoretically sound method for interpreting spectrochemical shifts in solvent mixtures and offers a methodology for separating dielectric enrichment, dielectric nonideality and specific interaction (i.e., hydrogen bonding) effects from one another.[11,15,17−24]

When a dipole is immersed in a binary solvent system with a polar and a nonpolar component, the solvent composition of its solvation sphere (the local composition) differs from the average solvent composition, even in the absence of specific solvent−solute interactions. The local composition is enriched in the polar solvent component because solvent dipole-solute dipole interactions are strongest between the solute and the polar component. The electrostatic work done on the system (i.e., the solvation energy) is more negative when the polar solvent component fills the solvation sphere. However, this process is entropically unfavorable because it decreases the entropy of mixing within the solvation sphere. The equilibrium local solvent composition is established when the decrease in electrostatic energy that results from an increase in the local concentration of the polar component is balanced by the increase in the local entropy caused by demixing. This nonspecific type of preferential solvation is referred to as dielectric enrichment. Because the electrostatic work can be cast in the framework of a dielectric continuum model of solvation, the equilibrium condition results in a thermodynamically rigorous expression for the local solvent composition, and relates the composition to the observed spectral shift of the dipolar solute.

The relevant time scale of dielectric enrichment is limited by two diffusive processes, the diffusion of the more polar solvent component toward the first solvation shell of the dipolar solute, and the diffusion of the less polar component away from the dipolar solute.[15] Intramolecular heteroexcimers (exciplexes) formed by charge transfer are excellent probes for dielectric enrichment because their long lifetimes[25] ensure that thermodynamic equilibrium is attained. The problem in utilizing these probes is that normally a minimum solvent polarity is required for the formation of these intramolecular heteroexcimers.[26] The ADMA [1-(9-anthryl)-3-(4-*N*,*N*-dimethylaniline)propane] molecule (Figure 1) can form an emissive heteroexcimer in solvents of low polarity, which is invaluable for measuring the local polarity in mixtures of polar and nonpolar solvents. ADMA is nonpolar in the ground state, but its excited-state heteroexcimer is very polar having a dipole moment of ∼12 D.[27] The position of the ADMA exciplex peak is therefore dependent upon the polarity of the solvent, and scales with the Lippert−Mataga polarity function.[11] The fluorescence lifetime of the ADMA heteroexcimer is very long[28−31] (∼150 ns in the absence of O_2) which makes it an ideal probe for local compositions.

In our previous work,[11] we have demonstrated that the application of eq 1 to spectroscopic data is limited to the cases where (a) the electronic structure of the solute molecule is not altered by its interaction with the surrounding solvent molecules and (b) the solvent mixture forms an ideal dielectric mixture, i.e., the Onsager polarity function of the mixture is a linear function of the composition. In this work, we measure the fluorescence spectra of ADMA in binary mixtures that approach ideal behavior,[15] namely hexane−tetrahydrofuran and hexane−dichloromethane. These results have been analyzed in terms of the theory of dielectric enrichment in order to determine the local composition. We have compared our results with the values predicted by eq 1, and have found that mixtures rarely exhibit behavior that is suitably ideal to justify the use of eq 1.

II. Dielectric Enrichment

Suppan's theory of dielectric enrichment has been discussed extensively.[11,15,16,18,19,22−24] In this section, we describe three independent methods for determining the central parameter of this theory, the index of preferential solvation (Z_{ps}). (For clarity we label these with subscripts 0, 1, and 2.) In the case of an ideal dielectric mixture, the local composition in the near vicinity of a dipolar solute is given by the following expression:

$$\frac{y_n}{y_p} = \frac{x_n}{x_p} e^{-Z_{ps}} \tag{2}$$

where x_n and x_p are the bulk, and y_n and y_p are the local mole fractions of the nonpolar and polar components of the solvent. Z_{ps} is referred to as the index of preferential solvation. In the single shell approximation $Z_{ps,0}$ is given by

$$Z_{ps,0} = \frac{3\mu^2 M \Delta F_{p-n}}{8\pi T R \delta r^6} \tag{3}$$

where M, R, and δ are the mean molar mass of the two solvent components, the gas constant and the mean density of the two solvent components, respectively. T is the absolute temperature of the system, μ is the dipole moment of the solute, ΔF_{p-n} is the difference between the Onsager polarity function of the polar and nonpolar components of the binary solvent mixture and $r = a + b$ where a is the radius of the solute and b is the radius of the solvent. The Onsager polarity function is given by the expression

$$F = \frac{2(\epsilon - 1)}{2\epsilon + 1} \tag{4}$$

These expressions provide a means of predicting the local solvent composition.

The second method for determining Z_{ps} utilizes the experimental data, and therefore the ideal mixture assumption is not required. (We denote the index of preferential solvation obtained by this method $Z_{ps,1}$.) $Z_{ps,1}$ is related to experimental data by employing the so-called "nonlinearity ratio" ρ_{exp}.[11,15] This quantity can be calculated from measured quantities using the expression

$$\rho_{exp} = \frac{2\int_0^1 (E_{exp} - E_{linear,bulk}) dx_p}{\Delta E_{p-n}} \tag{5}$$

where E_{exp} is the experimental peak energy of the fluorophore at bulk polar mole fraction x_p and $E_{linear,bulk} = x_p E_p + x_n E_n$ is the calculated peak energy of the fluorophore assuming it is dissolved in an ideal binary mixture at bulk polar mole fraction x_p. ΔE_{p-n} is the difference in peak energies in the neat polar and nonpolar solvents. Two factors contribute to the difference between E_{exp} and $E_{linear,bulk}$, preferential solvation and dielectric

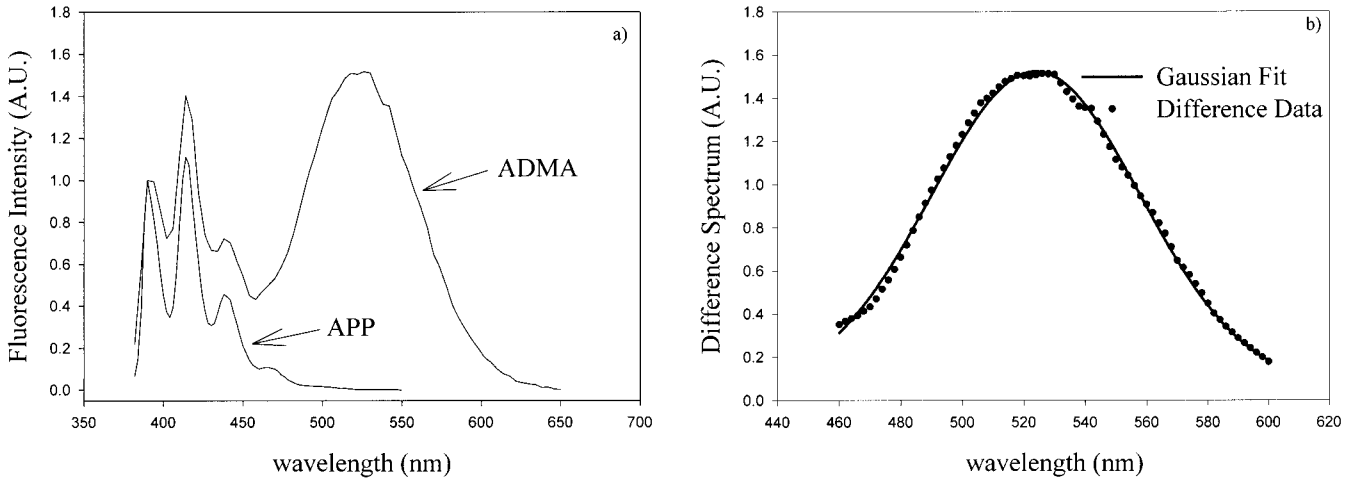

Figure 2. (a) Fluorescence spectra of ADMA and APP in tetrahydrofuran, illustrating their similarity in the 400−480 nm region. (b) Difference spectrum after subtraction of the APP spectrum from the ADMA spectrum. The circles are difference data points, and the line is a regression fit to a Gaussian peak shape. Center frequencies are taken from the results of the regression.

nonideality. We have demonstrated previously[11] that the experimental nonlinearity ratio ρ_{exp} can be expressed as the following sum:

$$\rho_{exp} = \rho_{ps} + \rho_{ni} \tag{6}$$

In which ρ_{ps} and ρ_{ni} are the contributions of preferential solvation and dielectric nonideality to the experimental nonlinearity ratio, respectively. The dielectric nonideality contribution ρ_{ni} can be calculated from experimental dielectric constant measurements using the expression

$$\rho_{ni} = \frac{2\int_0^1 (F_{exp} - F_{linear,bulk})dx_p}{\Delta F_{p-n}} \tag{7}$$

where F is given by eq 4, F_{exp} is calculated from measured dielectric constants of the mixtures, and $F_{linear,bulk}$ is calculated for an ideal dielectric mixture for which $F_{linear,bulk} = x_pF_p + x_nF_n$. Equations 5, 6, and 7 provide a means of calculating ρ_{ps} from experimental data. We have shown that when ρ_{ps} is less than 1, the relationship between ρ_{ps} and $Z_{ps,1}$ is well approximated by the expression[11,15]

$$\rho_{ps} = 0.31Z_{ps,1} \tag{8}$$

Equations 5−8 provide an independent method of calculating $Z_{ps,1}$ from experimental spectroscopic data.

Suppan's theory of dielectric enrichment also gives the relationship between experimental peak energies in ideal mixtures and the bulk composition of the mixture via eq 9,

$$\frac{1}{\Delta E} = -\frac{2a^3}{\mu^2 \Delta F_{p-n}}\left[1 - \frac{x_n e^{-Z_{exp}}}{x_p}\right] \tag{9}$$

in which ΔE is the measured peak shift relative to the peak energy measured in less polar component of the solvent mixture. A plot of $1/\Delta E$ vs x_n/x_p provides a second method for determining the index of preferential solvation from experimental data. We have approximated Z_{exp} as a sum of two contributions,

$$Z_{exp} = Z_{ps,2} + Z_{ni} \tag{10}$$

where $Z_{ps,2}$ is the contribution due to preferential solvation, and Z_{ni} is the contribution due to dielectric nonideality. Z_{ni} can be related to ρ_{ni} by an expression similar to eq 8, $\rho_{ni} = 0.31Z_{ni}$. In the following sections we use eqs 5 through 8 to obtain a measure of the $Z_{ps,1}$ from the experimental nonlinearity ratios. We have also obtained Z_{exp} directly from the data using eq 9 and use this to calculate the value of $Z_{ps,2}$ by subtracting the value of Z_{ni} determined from eq 8 and the experimental value for ρ_{ni}. We compare our two results with the theoretical prediction of $Z_{ps,0}$ using eq 3. Comparison of $Z_{ps,1}$ and $Z_{ps,2}$ demonstrates the validity of the approximations (eqs 6 and 10), and comparison of these with $Z_{ps,0}$ confirms dielectric enrichment as the mechanism of preferential solvation in hexane−dichloromethane and hexane−tetrahydrofuran binary mixtures.

TABLE 1: Peak Positions of the ADMA Sandwich Heteroexcimer (SH) Emission Peak in Pure Solvents and in Binary Hexane Mixtures[a]

solvent	SH peak (nm)	fitting error (nm)	peak energy (kJ/mol)
hexane	473.5	0.1	252.7
tetrahydrofuran (THF)	525.25	0.2	227.8
dichloromethane (DM)	526.4	0.2	227.3
11.8% THF/hexane	484.5	0.6	246.7
31.4% THF/hexane	496.7	0.2	240.9
48.9% THF/hexane	505.7	0.2	236.7
69.2% THF/hexane	516.25	0.2	231.8
89.7% THF/hexane	522.7	0.3	228.9
10.2% DM/hexane	481.0	0.4	248.7
18.8% DM/hexane	487.2	0.2	245.6
30.4% DM/hexane	493.1	0.4	242.6
50.5% DM/hexane	505.5	0.3	236.7
70.0% DM/hexane	513.0	0.4	233.2
91.0% DM/hexane	523.0	0.4	228.8

[a] The peak energies are given in nanometers and in kilojoules per mole. Mixture compositions are given in mole percent of the polar component. The error listed in the table is the standard error of the peak position from the nonlinear regression analysis. In all cases this error is small compared with the monochromator slit width of 1.5 nm, and the spectral resolution of 3 nm. Error bars in plots are based on the resolution uncertainty, which corresponds to an uncertainty of ±1.5kJ/mol.

III. Experimental Section

ADMA and APP [1-(9-anthryl)-3-(phenyl) propane, Figure 1] were synthesized according to methods outlined previously.[30] The solvents (*n*-hexane, dichloromethane, and tetrahydrofuran) were obtained in the purest form available from Aldrich. They were degassed by bubbling argon and used without further

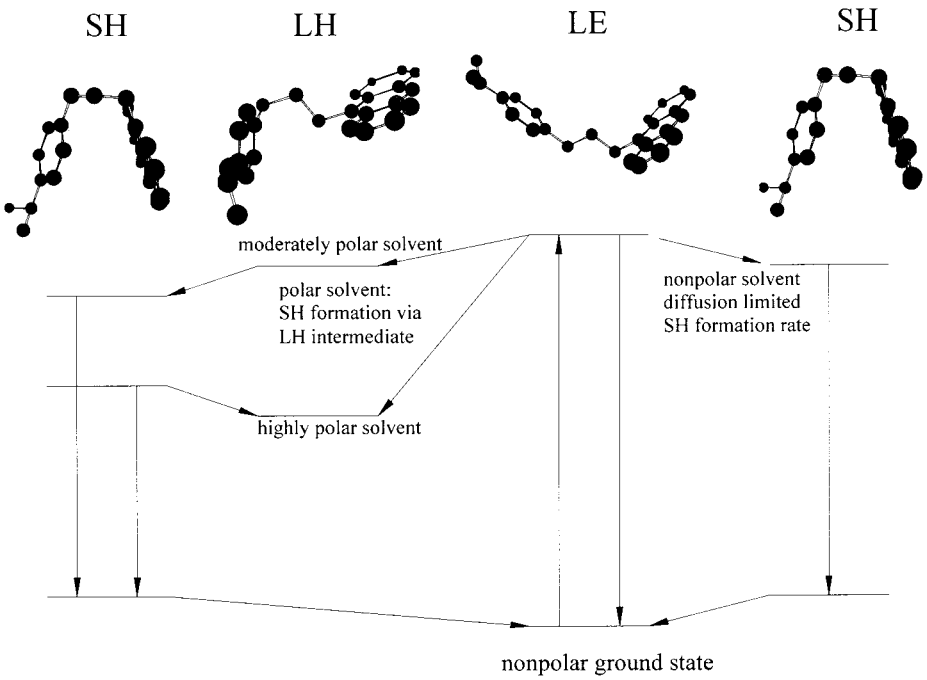

Figure 3. Energy level scheme for excited state isomerization kinetics of ADMA. The scheme demonstrates that sandwich heteroexcimer (SH) state formation is mediated by both solvent viscosity and solvent polarity. In polar solvents the favored pathway to the SH state is through the charge-separated loose heteroexcimer (LH) intermediate. The weakly emissive LH state becomes the low energy configuration in highly polar solvents. Solvent relaxation occurs after formation of the charge transfer state of the molecule.

purification. All solute concentrations were 10^{-5} M. The fluorescence spectra of the solutions where collected in a home-built scanning T-format fluorimeter.[11] The monochromator bandwidth was set at 1.5 nm giving 3 nm resolution. Samples were thermostated at 25 °C, unless noted otherwise. Dielectric constants of solvent mixtures were obtained from capacitance measurements using a thermostated capacitance cell and a capacitance instrument of our own design.[32] The solvent mixtures were prepared by weight.

The peak positions are obtained via the following procedure. The emission spectra of ADMA and APP are collected under identical conditions and the APP spectrum is subtracted from the ADMA spectrum. The resulting difference spectrum is representative of emission from the charge-transfer band.[11,30,31] The charge-transfer band can be modeled as a Gaussian peak using nonlinear regression (Sigmaplot) as shown in Figure 2b. The peak positions in the mixtures are given in Table 1 and it can be observed that the uncertainties are dominated by the 3 nm resolution of the fluorimeter. The peak positions obtained in the neat solvents are consistent with our previous results.[11]

IV. ADMA Charge Transfer State Formation

Figure 2a depicts the fluorescence spectrum of ADMA dissolved in tetrahydrofuran after irradiating the solution with 387 nm light. The spectrum has two distinct features. Structured emission below 450 nm that resembles anthracene emission and is observed in both ADMA and APP is assigned to the emission from the locally excited anthracene.[26] The broad emission in the 450−600 nm range which is only observed in the ADMA spectrum, has been assigned to emission from a folded charge-transfer exciplex.[33] Time-resolved studies of these features have elucidated the mechanism for charge transfer formation illustrated in Figure 3.[26,28,29,33,34] The figure shows three important configurations of ADMA: (1) the locally excited (LE) configuration, (2) the loose heteroexcimer (LH) configuration, and (3) the sandwich heteroexcimer(SH) configuration. The extended LE configuration is representative of the solute in the ground state. The SH configuration is the emissive charge-transfer excited state. This state is the low energy excited state conformation in solvents of modest polarity ($\epsilon < 20$). In nonpolar solvents the LE state must attain the folded conformation before charge transfer occurs causing the charge-transfer rate to be viscosity dependent.[30,31] An extended charge transfer configuration (the LH state) is the low energy conformation in highly polar solvents.[34,35] The LH state has a very low fluorescence quantum yield. This causes the charge transfer band shown in Figure 2a to be very weak in highly polar solvents such as methanol and acetonitrile.[34,35] In solvents of modest polarity, the LH state is formed directly from the LE state and the columbic attraction between the charge separated moieties results in the accelerated formation of the sandwich charge-transfer state.[28,34] Solvent polarity mediates the competition between the diffusive and accelerated pathways as illustrated in Figure 3.

The ADMA absorbance spectrum is relatively insensitive toward polarity demonstrating that the ground state has a low dipole moment. On the other hand, after excited state charge transfer occurs, the SH has a large dipole moment causing the energy of this configuration to be highly solvent dependent. The resulting solvatochromic shift is dynamic because the solvent dipole is created the instant charge transfer occurs. In neat solvents the dynamics is governed by solvent rotational motion, the time scale of which is smaller than the rate of charge transfer formation.[36−39] In solvent mixtures the solute is stabilized by the diffusion of the more polar compound into the solvation sphere of the SH configuration. This process is expected to occur on a nanosecond time scale,[15,20] complicating the interpretation of time-resolved emission from ADMA. However, the SH state is extremely long-lived (~150 ns in the absence of molecular oxygen).[28−30,34] Thus, the time-integrated charge-transfer emission peak energy is representative of the equilibrium stabilization

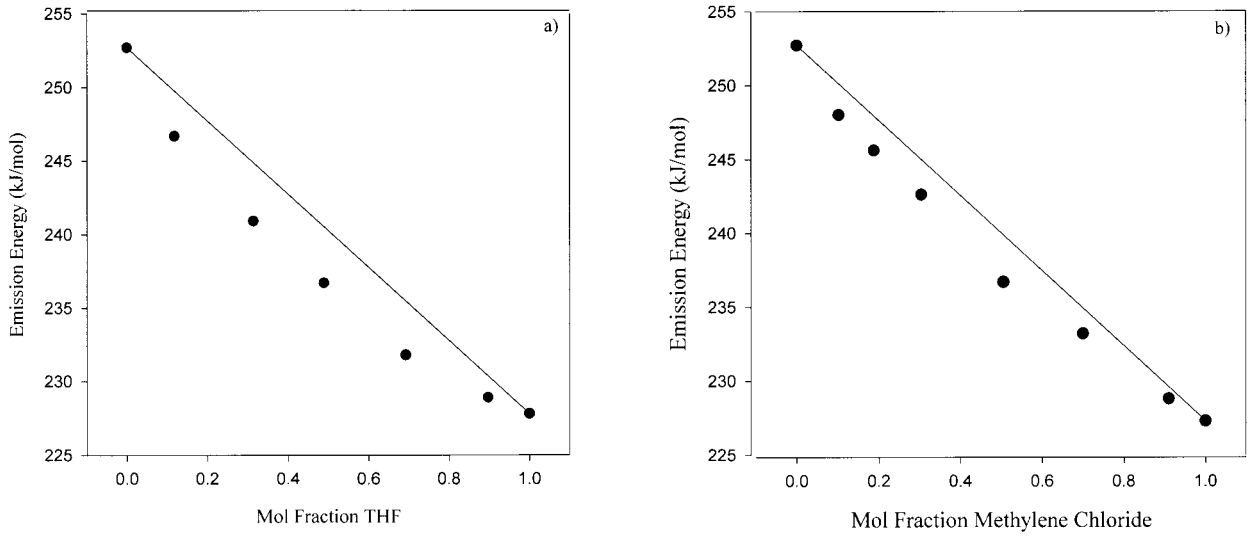

Figure 4. Plot of the ADMA sandwich heteroexcimer (SH) emission as a function of solvent composition in (a) hexane−tetrahydrofuran and (b) hexane−dichloromethane mixtures.

energy that the solute experiences and is an excellent probe for dielectric enrichment.[15]

V. Results and Analysis

Figure 4 plots the exciplex peak energies as a function of the bulk composition in two different binary solvent mixtures. In both cases, a deviation from linearity is observed. $Z_{ps,0}$ can be calculated directly from eq 3 using the ideal mixture-single shell approximation, and $Z_{ps,1}$ can be calculated from experimental data by applying eqs 5−8 after correcting for dielectric nonideality. In addition, eq 9 gives a direct method to determine $Z_{ps,2}$. We evaluate Z_{ps} by these methods in this section and discuss the relationship between each measure of Z_{ps}.

Calculation of $Z_{ps,0}$ from eq 3 requires the estimation of the solvent density, δ, solvent molar mass, M, and the distance between the cavity center and the first solvation sphere, r. We have shown that the bulk-mole-fraction-weighed molar mass and mixture densities at each composition give realistic estimates for this parameter.[11] Table 2 presents $Z_{ps,0}$ values determined using three separate estimates of r. We have presented this comparison because it is the parameter whose value most strongly influences $Z_{ps,0}$. As before,[11] we suggest that the most objective measure of r is the bulk-mole-fraction-weighed (bmfw) van der Waals radius of the solvent. We have also calculated $Z_{ps,0}$ using the van der Waals radii of the pure components[40] because these values must bracket the correct radius. Table 2 indicates that the overall average value of $Z_{ps,0}$ is 0.34 (±3%) for hexane−tetrahydrofuran mixtures and 0.34 (±7%) for hexane−dichloromethane mixtures. These values are nearly identical to values calculated from bmfw parameters. If the uncertainty in the dipole moment is also considered, the average bmfw values are $Z_{ps,0} = 0.34 \pm 0.03$ for hexane−tetrahydrofuran mixtures and $Z_{ps,0} = 0.33 \pm 0.04$ for hexane−dichloromethane mixtures. It should be born in mind that eq 3 assumes that the mixture is an ideal dielectric and the resulting $Z_{ps,0}$ values only reflect the contribution of preferential solvation to the solute charge-transfer emission peak energy.

To effectively compare $Z_{ps,0}$ with the experimentally determined indices of preferential solvation the dielectric properties of the binary mixtures have to be well characterized. We have measured the dielectric constant of these mixtures at 25 °C, and the results have been fit to the following empirical composition dependences: $\epsilon = 1.882 + 3.218x_p - 0.690x_p^2 + 2.977x_p^3$ for hexane−tetrahydrofuran mixtures and $\epsilon = 1.882 + 3.933x - 5.771x_p^2 + 8.969x_p^3$ for hexane−dichloromethane

TABLE 2: Calculation of $Z_{ps,0}$ for THF−Hexane and DM−Hexane Mixtures[a]

mol % THF	radius value	*b* (Å)	*M* (kg/mol)	δ (kg/m^3)	Z
11.8%	THF radius	2.20	0.0845	681.4	0.49
	hexane radius	2.58	0.0845	681.4	0.35
	bmfw radius	2.54	0.0845	681.4	0.36
31.4%	THF radius	2.20	0.0818	725.5	0.44
	hexane radius	2.58	0.0818	725.5	0.32
	bmfw radius	2.46	0.0818	725.5	0.35
48.9%	THF radius	2.20	0.0793	764.9	0.41
	hexane radius	2.58	0.0793	764.9	0.29
	bmfw radius	2.39	0.0793	764.9	0.34
69.2%	THF radius	2.20	0.0764	818.6	0.37
	hexane radius	2.58	0.0764	818.6	0.26
	bmfw radius	2.32	0.0764	818.6	0.33
89.7%	THF radius	2.20	0.0736	856.8	0.34
	hexane radius	2.58	0.0736	856.8	0.24
	bmfw radius	2.24	0.0736	856.8	0.33
	mean parameters	2.39	0.0791	767.4	0.34
mol % DM	radius value	*b* (Å)	*M* (kg/mol)	δ (kg/m^3)	Z
10.2%	DM radius	2.05	0.0860	722.4	0.58
	hexane radius	2.58	0.0860	722.4	0.36
	bmfw radius	2.53	0.0860	722.4	0.38
18.8%	DM radius	2.05	0.0859	779.3	0.54
	hexane radius	2.58	0.0859	779.3	0.33
	bmfw radius	2.48	0.0859	779.3	0.36
30.4%	DM radius	2.05	0.0858	855.7	0.49
	hexane radius	2.58	0.0858	855.7	0.30
	bmfw radius	2.42	0.0858	855.7	0.35
50.5%	DM radius	2.05	0.0855	989.2	0.42
	hexane radius	2.58	0.0855	989.2	0.26
	bmfw radius	2.31	0.0855	989.2	0.33
70%	DM radius	2.05	0.0853	1118.3	0.37
	hexane radius	2.58	0.0853	1118.3	0.23
	bmfw radius	2.21	0.0853	1118.3	0.32
91%	DM radius	2.05	0.0850	1257.4	0.33
	hexane radius	2.58	0.0850	1257.4	0.20
	bmfw radius	2.10	0.0850	1257.4	0.32
	mean parameters	2.32	0.0855	985.6	0.33

[a] The molar mass (M) and the density (δ) are the mole fraction weighted averages of the pure components. In all cases, the ADMA van der Waals radius of 4.32 Å is used as the cavity radius. Z is calculated for three values of the solvent shell halfwidth including the bulk mole fraction weighed (bmfw) radius. Z has also been calculated for mean (arithmetic average) parameter values.

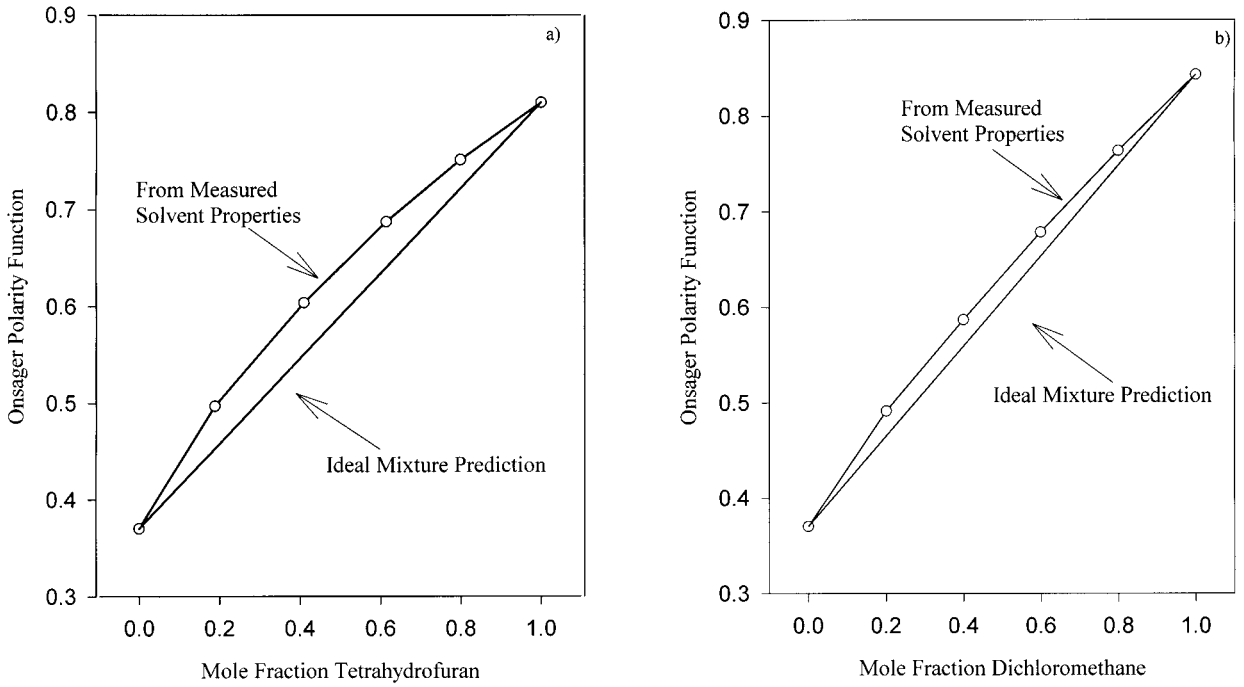

Figure 5. Solvent polarity function calculated from measured values of permittivity (ϵ) for (a) hexane−tetrahydrofuran and (b) hexane−dichloromethane mixtures versus solvent composition. The straight line represents the prediction for an ideal dielectric mixture.

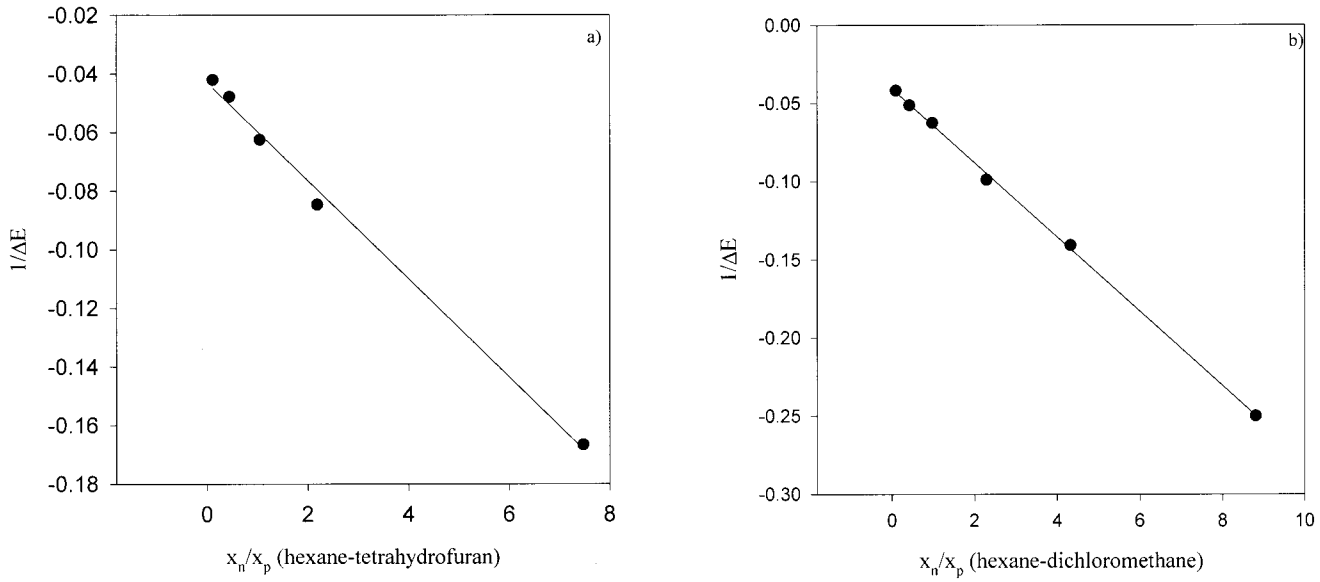

Figure 6. Inverse peak shift (measured against the hexane peak position) of the ADMA SH emission versus solvent composition. Deviation from linearity occurs when specific interactions contribute to preferential solvation.

mixtures. Using eq 5 and the data in Figure 4 and Table 1, we obtain the nonlinearity ratios $\rho_{exp} = 0.15 \pm 0.02$ and $\rho_{exp} = 0.25 \pm 0.02$ for hexane−dichloromethane and hexane−tetrahydrofuran mixtures, respectively. The composition dependent Onsager polarity functions determined from experimental dielectric constant values are shown in Figure 5. The nonideality contributions calculated from eq 7 reflect the integral of the difference between the ideal and measured curves. Their values are $\rho_{ni} = 0.078$(hexane−dichloromethane) and $\rho_{ni} = 0.160$ (hexane−tetrahydrofuran). Using eq 8 and the above values of ρ_{exp} and ρ_{ni} we find $Z_{ps,1} = 0.23 \pm 0.07$ for hexane−dichloromethane, and $Z_{ps,1} = 0.29 \pm 0.02$ for hexane−tetrahydrofuran. These results agree with the values of $Z_{ps,0}$ (the single- shell, ideal mixture approximation predictions) within the uncertainties of the determinations.

Figure 6 exhibits linear plots of $1/\Delta E$ against x_n/x_p for both mixture systems. From the fitting parameter values we obtain $a = 4.34$ Å and $Z_{exp} = 0.94 \pm 0.13$ for hexane−tetrahydrofuran mixtures and $a = 4.36$ Å and $Z_{exp} = 0.54 \pm 0.06$ for hexane−dichloromethane mixtures. The experimental value of a is extremely close to the van der Waals radius of ADMA. This demonstrates the utility of eq 9. Using the expression $\rho_{ni} = 0.31Z_{ni}$ and the experimentally determined values of ρ_{ni} described above, we find $Z_{ni} = 0.25$ (hexane−dichloromethane) and $Z_{ni} = 0.52$ (hexane−tetrahydrofuran). Using eq 10, we find $Z_{ps,2} = 0.29 \pm 0.06$ (hexane−dichloromethane) and $Z_{ps,2} = 0.43 \pm 0.13$ (hexane−tetrahydrofuran). Again these values are in agreement with the values of $Z_{ps,0}$ and $Z_{ps,1}$ within the uncertainty of the deteminations.

TABLE 3: Local Mole Fraction of the Polar Solvent Component around the ADMA Sandwich Heteroexcimer (SH) Dissolved in Hexane−Tetrahydrofuran or Hexane−Dichloromethane Mixtures Calculated Using Equation 2 for Three Different Z_{ps} Values[a]

$x_{p,tetrahydrofuran}$	$y_{p,1}$ (from $Z_{ps,1}$)	$y_{p,2}$ (from $Z_{ps,2}$)	$y_{p,0}$ (from $Z_{ps,0}$)	$y_{p,linear}$ (from eq 1)
0.118	0.152	0.171	0.161	0.241
0.314	0.380	0.413	0.394	0.474
0.489	0.561	0.595	0.573	0.643
0.692	0.750	0.775	0.758	0.839
0.897	0.921	0.930	0.924	0.937
$x_{p,dichloromethane}$	$y_{p,1}$ (from $Z_{ps,1}$)	$y_{p,2}$ (from $Z_{ps,2}$)	$y_{p,0}$ (from $Z_{ps,0}$)	$y_{p,linear}$ (from eq 1)
0.102	0.125	0.131	0.142	0.210
0.304	0.354	0.369	0.383	0.398
0.505	0.562	0.577	0.587	0.630
0.700	0.746	0.757	0.763	0.768
0.910	0.927	0.931	0.933	0.941

[a] The mean parameter values of $Z_{ps,0}$ given in Table 2 were used to find $y_{p,0}$. The local composition y_p has also been calculated from eq 1.

VI. Discussion

Table 3 presents local polar mole fractions calculated using the different Z_{ps} values. From these results it is clear that the excess local polar mole fraction $(y_p - x_p)/x_p$ is the greatest at lowest bulk mole fraction, with the local composition exhibiting nearly 30% excess polar mole fractions over the bulk composition. The variation between the local composition values calculated using different approaches within the theory of dielectric enrichment is less than 7% across the entire range of bulk compositions. Thus the variations in the values of Z_{ps} calculated by different methods result in small variations in local composition. However, the local compositions from dielectric enrichment theory are substantially lower than local compositions determined from spectral peak shifts using the linear approximation of eq 1, with the linear approximation overpredicting the local composition by as much as 50%. In our previous paper, concerning hexanes−ethanol mixtures[11] we showed that eq 1 overpredicted the local polar mole fraction by up to 100%. The overprediction of eq 1 decreases as the mixture becomes more nearly ideal (i.e., the overprediction follows the trend ethanol−hexane > tetrahydrofuran−hexane > dichloromethane−hexane). This clearly indicates that eq 1 becomes more appropriate as the mixture approaches an ideal dielectric mixture. Nevertheless, the nonideality of tetrahydrofuran−hexane and dichloromethane−hexane mixtures still makes a sizable contribution to the observed spectrochemical shift of a fluorescent dipole dissolved in these solvents.

It is important to note that Suppan's ideal dielectric, single shell approximate form of dielectric enrichment theory does predict a linear dependence of peak shift on local mole fraction, consistent with eq 1. However, Suppan does not use eq 1 as a measure of local composition. Rather, the local composition is determined by first calculating $Z_{ps,0}$ which is based on thermodynamic arguments. Thus, if Suppan's ideal dielectric single shell theory is used to calculate the local composition of a nonideal dielectric mixture around a dipolar solute, the resulting local compositions are correct. However if the resulting local compositions are used in eq 1 to calculate the peak shift of the solute, the calculated shift will underpredict the observed shift. To predict the correct shift, one needs to also calculate ρ_{ni} from measured mixture dielectric properties using eq 8. Then an effective index of preferential solvation, $Z_{ps,eff}$ must be constructed using the expressions $\rho_{ni} = 0.31Z_{ni}$ and $Z_{ps,eff} = Z_{ps,0} + Z_{ni}$. Using this value of $Z_{ps,eff}$ in eq 2, the "effective local composition" is found, and the linear prediction of eq 1 using the resulting local mole fractions will properly predict the observed peak shift. Note however that the effective local composition does not properly reflect the true composition of the solute solvation sphere unless Z_{ni} is nearly zero. Conversely, local mole fractions derived from experimental peak shifts and eq 1 reflect contributions of both preferential solvation due to dielectric enrichment and mixture dielectric nonideality.

The local compositions derived from dielectric enrichment theory given in Table 3 vary by less than 10% from one another. Using the 10% variation as a benchmark, we have found that Z_{ni} must be less than ~0.1 ($\rho_{ni} < 0.03$) in order for eq 1 to give a local polar mole fraction that is within 10% of the value determined from the full dielectric enrichment treatment. These results are in agreement with expectation. Hexanes−ethanol mixtures are highly nonideal therefore any deviation of the peak energy from linearity in composition is a sum of both nonideal and preferential solvation effects. Since the contribution from dielectric nonideality is significant in hexanes−ethanol mixtures, eq 1 over predicts the local composition. The dielectric properties of hexane−tetrahydrofuran and hexane−dichloromethane mixtures are closer to ideal behavior, and the values predicted from eq 1 begin to approach dielectric enrichment calculations. These results address the objection raised by Ben-Naim,[9,10] namely the theoretical basis of eq 1. In the case of electronic spectra, eq 1 is only valid for spectral shifts of dipolar molecules dissolved in ideal dielectric mixtures whose molecular structure is not affected by polarity. From a practical standpoint, it is useful to know when these conditions are satisfied. Dielectric nonideality is the result of differences in interactions between one solvent component with itself and interactions of the two components of the solvent with each other. Thus, it stands to reason that solvent mixtures of components with similar dielectric constants will exhibit behavior that is more nearly ideal. On the other hand, solutes will only respond to variations in solvent compostion when those variations influence the mixture dielectric constant. To date we have studied mixtures composed of solvents whose dielectric constants differ by as little as about 5 units. In these cases we still observe a substantial influence of dielectric nonideality on solvent−solute interactions, and a complete dielectric enrichment treatment is necessary to correctly characterize the local composition. Thus, from a practical standpoint, dielectric nonideality can be expected to occur in mixtures that will typically be useful for chemical processing such as chromatography and extraction. In general, therefore, determination of local composition by spectroscopic methods requires a precise knowledge of the composition dependence of the dielectric properties of the binary mixture.

Acknowledgment. This research was supported by the National Science Foundation (NSF CHE-9508744) and the University of Missouri Research Board.

References and Notes

(1) Marcus, Y. *Aust. J. Chem.* **1983**, *36*, 1719−31.
(2) Acree, W. E.; Tucker, S. A.; Wilkins, D. C. *J. Phys. Chem.* **1993**, *97*, 11199−11203.
(3) Acree, W. E.; Tucker, S. A.; Wilkins, D. C. *J. Phys. Chem.* **1994**, *98*, 2537−2544.
(4) Bosch, E.; Roses, M. *J. Chem. Soc., Faraday Trans.* **1992**, *88*, 3541−3546.
(5) Banerjee, D.; Laha, A. K.; Baghchi, S. *J. Chem. Soc., Faraday Trans.* **1995**, *91*, 631−636.
(6) Banerjee, D.; Baghchi, S. *J. Photochem. Photobiol. A: Chem.* **1996**, *101*, 57−62.
(7) Chatterjee, P.; Baghchi, S. *J. Phys. Chem.* **1991**, *95*, 3311−3314.

(8) Szpakowska, M.; Nagy, O. B. *J. Chem. Soc., Faraday Trans. 1* **1989**, *85*, 2891.
(9) Ben-Naim, A. *Cell Biophys.* **1988**, *12*, 255−269.
(10) Ben-Naim, A. *Statistical Mechanics for Chemists and Biochemists*; Plenum: New York, 1992.
(11) Khajehpour, M. H.; Kauffman, J. F. *J. Phys. Chem. A* **2000**, *104*, 7151−7159.
(12) Mataga, N.; Kubota, T. *Molecular Interactions and Electronic Spectra*; Marcel Dekker: New York, 1970.
(13) Midwinter, J.; Suppan, P. *Spectrochim. Acta* **1969**, *25A*, 953−958.
(14) Nitsche, K.-S.; Suppan, P. *Chimia* **1982**, *36*, 346−348.
(15) Suppan, P. *J. Chem. Soc., Faraday Trans. 1* **1987**, *83*, 495−509.
(16) Suppan, P. *J. Photochem. Photobiol. A: Chem.* **1990**, *50*, 293−330.
(17) Lerf, C.; Suppan, P. *J. Chem. Soc., Faraday Trans.* **1992**, *88*, 963−969.
(18) Cichos, F.; Willert, A.; Rempel, U.; Borczyskowski, C. v. *J. Phys. Chem. A* **1997**, *101*, 8179−8185.
(19) Zurawski, W. P.; Scarlata, S. F. *J. Phys. Chem.* **1992**, *96*, 6012−6016.
(20) Petrov, N. K.; Wiessner, A.; Staerk, H. *J. Chem. Phys.* **1998**, *108*, 2326−2330.
(21) Petrov, N. K.; Wiessner, A.; Fiebig, T.; Staerk, H. *Chem. Phys. Lett.* **1995**, *241*, 127−132.
(22) Schatz, T. R.; Kobetic, R.; Piotrowiak, P. *J. Photochem. Photobiol. A: Chem.* **1997**, *105*, 249−254.
(23) Raju, B. B.; Costa, S. M. B. *Phys. Chem. Chem. Phys.* **1999**, *1*, 3539−3547.
(24) Ghoneim, N. *Spectrochim. Acta A* **2000**, *56* (A), 1003−1010.
(25) Gordon, M.; Ware, W. R. *The Exciplex*; Academic Press: New York, 1975; p 372.
(26) Masaki, S.; Okada, T.; Mataga, N.; Sakata, Y.; Misumi, S. *Bull. Chem. Soc. of Jpn.* **1976**, *44*, 1277−1283.
(27) Baumann, W.; Frohling, J.-C.; Brittinger, C.; Okada, T.; Mataga, N. *Ber. Bunsen-Ges. Phys. Chem.* **1988**, *92*, 700−706.
(28) Migita, M.; Okada, T.; Mataga, N.; Nakashima, N.; Yoshihara, K.; Sakata, Y.; Misumi, S. *Chem. Phys. Lett.* **1980**, *72*, 229−232.
(29) Migita, M.; Okada, T.; Mataga, N.; Nakashima, N.; Yoshihara, K.; Sakata, Y.; Misumi, S. *Bull. Chem. Soc. of Jpn.* **1981**, *54*, 3304−3311.
(30) Khajehpour, M.; Kauffman, J. F. *Chem. Phys. Lett.* **1998**, *297*, 141.
(31) Wang, Y.; Crawford, M. C.; Eisenthal, K. B. *J. Am. Chem. Soc.* **1982**, *104*, 5874−5878.
(32) Liu, C.; Kauffman, J. F. *Rev. Sci. Instr.* **1996**, *67*, 525−529.
(33) Chuang, T. J.; Cox, R. J.; Eisenthal, K. B. *J. Am. Chem. Soc.* **1974**, *96*, 6828−6831.
(34) Okada, T.; Migita, M.; Mataga, N.; Sakata, Y.; Misumi, S. *J. Am. Chem. Soc.* **1981**, *103*, 4715−4720.
(35) Crawford, M. K.; Wang, Y.; Eisenthal, K. B. *Chem. Phys. Lett.* **1981**, *79*, 529−533.
(36) Maroncelli, M. *J. Mol. Liq.* **1993**, *57*, 1−37.
(37) Maroncelli, M.; Kumar, V. P.; Papazyan, A. *J. Phys. Chem.* **1993**, *97*, 13−17.
(38) Jimenez, R.; Fleming, G. R.; Kumar, P. V.; Maroncelli, M. *Nature* **1994**, *369*, 471−473.
(39) Reynolds, L.; Gardecki, J. A.; Frankland, S. J. V.; Horng, M. L.; Maroncelli, M. *J. Phys. Chem.* **1996**, *100*, 10337−10354.
(40) Dean, J. A. *Lange's Handbook of Chem.*; McGraw-Hill: New York, 1992.